PAPER

Check for updates

Fully inkjet-printed distance-based paper microfluidic devices for colorimetric calcium determination using ion-selective optodes†

Hiroyuki Shibata, Yuki Hiruta [ID] and Daniel Citterio [ID] *

Although the determination of calcium ions (Ca^{2+}) is of high importance to monitor water hardness, currently available devices for on-site analysis suffer from a lack of user-friendliness and sensitivity. This work demonstrates fully inkjet-printed and low-cost microfluidic paper-based analytical devices (µPADs) for the simple naked-eye colorimetric determination of calcium ions (Ca^{2+}) in drinking and tap water samples. The quantification of Ca^{2+} relies on visual readout of the length of a colour-changed detection channel modified with ionophore-doped ion-selective optode nanospheres (nano-optodes), eliminating the requirement of a scanner or a camera. All fabrication steps for deposition of assay reagents have been performed by means of a simple desktop thermal inkjet printer, which is expected to contribute to highly batch-to-batch reproducible device preparation. The detectable Ca^{2+} concentrations between 0.05 mmol L^{-1} and 5 mmol L^{-1} cover the range recommended by the International Organization for Standardization (0.05–2.5 mmol L^{-1}) and the World Health Organization (WHO) guideline for Ca^{2+} quantification in drinking water (less than 5 mmol L^{-1}). The lowest concentration of Ca^{2+} detectable by the naked eye was found to be 0.05 mmol L^{-1}, which is below the value achieved with previously reported paper-based devices. µPAD quantified Ca^{2+} concentrations in tap or drinking waters were within 15% error of the results obtained with a classical complexometric titration. Hence, distance-based µPADs relying on nano-optodes are sensitive and reproducible tools for equipment-free on-site assaying of Ca^{2+} in real samples.

Introduction

Calcium (Ca) is found as an important trace mineral and nutrient in natural or drinking waters, and together with magnesium (Mg) determines the water hardness. The World Health Organization (WHO) published a report on the public health significance of water hardness, addressing its benefits and risks.[1] Although no strict criteria for Ca^{2+} levels in the context of drinking water quality have been defined in this guideline, the WHO alternatively established a recommen-

Department of Applied Chemistry, Keio University, 3-14-1 Hiyoshi, Kohoku-ku, Yokohama 223-8522, Japan. E-mail: citterio@applc.keio.ac.jp; Fax: +81 45 566 1568 ; Tel: +81 45 566 1568

†Electronic supplementary information (ESI) available: Nano-optode preparation, wax pattern design, procedure for obtaining colorimetric response profiles, complexometric titration of water samples, optimisation of printing cycles for nano-optodes, wax barrier tolerance against leakage, optimisation of printing cycles for pH-buffering reagents and $MgCl_2$, comparison between different batches of µPADs, comparison between software-assisted readout and readouts by untrained users, quantification of Ca^{2+} with commercial paper dipsticks, selectivity evaluation, method comparison of distance-based µPADs with complexometric titration, and evaluation of Ca^{2+} adsorption to paper substrate and error of observer tests. See DOI: 10.1039/c8an02146e

dation for Ca^{2+} levels in drinking water to be below 5 mmol L^{-1} and a taste threshold for Ca^{2+} in the range of 2.5–7.5 mmol L^{-1}.[1] Quantitative and selective quantification of Ca relies on a wide variety of classical analytical methods, such as complexometric titration, spectrophotometry and atomic absorption spectrometry (AAS).[1–3] As a standardised protocol provided by the International Organization for Standardization, classic complexometric titrations using cation-responsive chromogens and chelating reagents are applied to the direct determination of calcium levels in the range of 0.05–2.5 mmol L^{-1}.[4] While this analytical approach is inexpensive and relatively simple, it is difficult to be adapted to on-site or in-field assays because of the necessity of specific experimental equipment (*e.g.* burette) and the multistep nature of the assay including sample pretreatment with a strongly basic solution (pH ≈ 12) for masking interfering cations.[4,5] On the other hand, spectrophotometry and AAS allow for selective, sensitive, and reliable measurement of the target ions of interest. However, they are expensive, labour intensive, and complicated for untrained users.

Since Whitesides' research group first established the concept of microfluidically patterned paper,[6,7] microfluidic paper-based analytical devices (µPADs) have emerged as a new

class of analytical platform over conventional paper strips for point-of-need analysis.[3,8–14] In this context, the naturally porous structure of cellulosic paper plays an important role as a sustainable, inexpensive, ready-to-use, and safely disposable substrate platform for (semi-)quantitative assays applied to both clinical and environmental monitoring. Passive sample transportation through capillary forces enables sophisticated (bio)chemical assays, including sample pretreatment steps, and µPADs have evolved into analytical tools helping to overcome some limitations of conventional analytical instruments in terms of cost, portability and user-friendliness. Colorimetric µPADs are of particularly high interest, because they allow for unaided eye observable quantitative signal readout.[15] Not surprisingly, various metal ions (especially heavy metals) have been colorimetrically determined on µPADs due to the wide availability of classical colorimetric indicators.[3,12–14,16–20] With regard to the colorimetric detection of Ca^{2+}, complexometric titration reagents, such as chelating reagents, cation-responsive chromogens, and masking reagents, have typically been adapted to the cellulosic substrate.[21–23] Kaneta's research group for example, fully integrated the classical complexometric titration system into a µPAD for the visual determination of Ca^{2+} and Mg^{2+} in natural or drinking waters without the requirement for burettes and optical signal quantification tools (e.g. camera, scanner).[22] Nevertheless, paper-based assays for visual detection of Ca^{2+} in drinking water and tap water suffer from relatively poor limits of detection (LOD), with an LOD of 0.21 mmol L^{-1} reported for a µPAD relying on software-assisted colorimetric readout,[21] or of 5 mmol L^{-1} by naked eye visual detection.[22]

As one of the sophisticated optical chemical sensors targeting ionic species, ionophore-based ion-selective optodes (ISOs) continue to attract significant attention.[24–26] Classical ISOs are typically composed of lipophilic sensing components, such as a pH indicator as optical transducer (chromoionophore), an ion-specific ligand (ionophore), and an organic salt additive (ion-exchanger), embedded into a plasticised polymeric membrane.[24,27] Due to the versatile capabilities of ISOs, their detection function has been integrated into cellulosic material platforms, such as a cotton thread[28] and paper substrates.[29–36] More recently, our research group introduced the classical polymer film-based ISOs into µPADs with the aid of inkjet printing technology.[29] In a later stage, we reported the use of inkjet-generated polymeric particle-based ISOs on paper strips.[30] Meyerhoff's research group on the other hand, first established a new class of ISOs without the conventional plasticised polymeric materials on paper substrates,[31] and first applied inkjet printing technology for the deposition of the corresponding ISO components.[32–34] Although paper-based ISOs have served to determine various electrolytes, they require optical signal readout tools (e.g. scanner, camera, reflectometry). Only in 2018, Henry's and Bakker's research groups succeeded in the elimination of the conventional colour intensity or colour hue readout by adapting a distance-based signal readout motif to ISOs with micelle-based nano-spheres (nano-optodes) pipetted onto µPADs.[35] Nevertheless,

inkjet printing technology has to best of our knowledge never been applied to the highly-reproducible and well-defined deposition of all assay reagents onto practical µPADs.

The present work demonstrates distance-based µPADs for the naked-eye quantification of Ca^{2+} in drinking or tap waters with high batch-to-batch reproducibility and assay accuracy without any external equipment. For this purpose, nano-optodes composed of the surfactant Pluronic® F-127 have been applied to the fabrication of distance-based µPADs by means of inkjet printing technology. Notably, the nano-optodes no longer require the use of volatile organic solvents in the paper device fabrication process (e.g. tetrahydrofuran, cyclohexanone).[25,37,38] Therefore, it is possible to use simple desktop thermal inkjet printing for their deposition onto wax-patterned paper substrates. All fabrication steps leading to the distance-based µPADs, from the microfluidic patterning of the paper substrate (wax printing) to the deposition of all required assay reagents (inkjet printing), were performed with standard printing technology, which is expected to contribute to highly reproducible and scalable fabrication with minimum consumption of chemical reagents.[39,40] Additionally, the developed µPADs show a lower naked-eye observable LOD (0.05 mmol L^{-1}) than a commercial colorimetric paper dipstick (0.1 mmol L^{-1}), and they are applicable to practical sample analysis of Ca^{2+} with sufficient accuracy (no more than 15% error).

Materials and methods

Reagents and instruments

All reagents were used without further purification. Chromoionophore I (CH1), calcium ionophore IV and tetramethylammonium hydroxide pentahydrade (TMAOH) were purchased from Sigma-Aldrich (St Louis, MO). Pluronic® F-127 (F127) was purchased from BASF (Ludwigshafen, Germany). Tetrahydrofuran (THF) was purchased from Kanto Chemical (Tokyo, Japan). Bis(2-ethylhexyl) sebacate (DOS), sodium chloride (NaCl), potassium chloride (KCl), calcium chloride dihydrate ($CaCl_2 \cdot 2H_2O$) and magnesium chloride hexahydrate ($MgCl_2 \cdot 6H_2O$) were purchased from Wako Pure Chemical Industries (Osaka, Japan). N-(2-Hydroxyethyl)-1-piperazineethanesulfonic acid (HEPES), sodium tetrakis[3,5-bis(trifluoromethyl)phenyl]borate (NaTFPB), 2-hydroxy-1-(2-hydroxy-4-sulfo-1-naphthylazo)-3-naphthoic acid (NN) and 0.01 N EDTA (ethylenediaminetetraacetate) titration solution ($f = 1.001$) were purchased from Dojindo Laboratories (Kumamoto, Japan). Colorimetric paper dipsticks for Ca^{2+} assays were purchased from Merck Milllipore (Darmstadt, Germany).

Ultrapure water (>18 MΩ cm) was obtained from a PURELAB flex water purification system (ELGA, Veolia Water, Marlow, U.K.) and used for the preparation of all solutions. Advantec No. 5C filter paper was purchased from Toyo Roshi (Tokyo, Japan). Hot lamination films (150 µm thickness, film material: polyethylene terephthalate and polyvinyl alcohol as a thermoplastic adhesive) were obtained from Jointex (Tokyo, Japan). For inkjet printing of the reagents for Ca^{2+} detection, a

thermally-actuated Canon iP2700 inkjet printer (Canon, Tokyo, Japan) was used. For this purpose, the standard colour cartridge of the Canon printer was cut open and the sponge inside and colour inks were removed, followed by washing with copious amounts of deionised water. Dynamic light scattering (DLS) measurements to evaluate the hydrodynamic diameter of nano-optodes were performed by a Zetasizer Nano ZS from Malvern (Worcestershire, UK). Optical microscope images were acquired on a DVM2500 digital microscope (Leica, Wetzlar, Germany).

Preparation of Ca^{2+}-selective nano-optode suspension

The preparation of the ion-selective optode nanospheres (nano-optodes) according to previously published articles[37,38] and the evaluation of their physical properties by DLS are described in the ESI and in Fig. S1.†

Device fabrication for distance-based Ca^{2+} quantification

A ColorQube 8570 printer (Xerox, Norwalk, CT, USA) was used to pattern wax barriers on filter paper sheets cut into A4-size before use. 32 identical wax patterns designed in PowerPoint (Microsoft) were transferred to one single sheet of paper, as shown in Fig. S2 in the ESI.† For melting the wax into the depth of the paper to produce hydrophobic barriers, printed patterns were heated on a hot plate (Nissin NHS-450ND, Nissinrika, Tokyo, Japan) at 150 °C for 3 min. To prevent contamination from paper feeding rollers of the printer during inkjet printing steps, the back side of wax-patterned paper was laminated. The wax-patterned and back side-laminated paper substrates were then subjected to reagent deposition to obtain the distance-based µPADs for colorimetric determination of Ca^{2+} as described below and illustrated in Fig. 1.

As sample pretreatment reagents, pH-buffering solution (250 mmol L^{-1} HEPES-TMAOH buffer, pH 7.0) and 10 mmol L^{-1} aqueous $MgCl_2$ solution, were separately inkjet-deposited from a black ink cartridge in 1 and 3 print cycles, respectively. Then, Ca^{2+}-selective nano-optodes were inkjet-printed from a magenta ink cartridge in 20 printing cycles. After the inkjet printing step, the printed sides of the µPADs were laminated with exception of the sample inlet area to limit evaporation of sample liquid during assays.

Distance-based Ca^{2+} assay with µPADs

30 µL of aqueous $CaCl_2$ solution was applied to the sample inlet of the µPAD, followed by incubation under ambient condition to perform the nano-optode reaction (45 min). The generated colorimetric signals were captured as JPEG images of 600 dpi resolution with a Canoscan 9000F MarkII colour scanner (Canon, Tokyo, Japan). The obtained images were processed by separating the colour into the red, green and blue channels. The red channel was used to quantify the colorimetric change of paper devices. The length of the colour-changed nano-optode section of the detection channel was measured with the ImageJ software (NIH, Bethesda, MD). The colorimetric response profile recorded along the detection channel shown in Fig. S3† was obtained by using the data smoothing function of ImageJ. It is noted here that the distance-based µPADs are intended for equipment-free naked-eye signal readout. The use of scanned images and image processing software exclusively serves the purpose of device characterization. Curve fitting of the experimentally acquired response data was performed with the Igor Pro 4.01 software package (WaveMetrics, Lake Oswegeo, OR) based on a sigmoidal equation and estimates for the concentration of Ca^{2+} were obtained with the "Solver" function of Excel (Microsoft).

Ca^{2+} assay in water samples

All used mineral waters were purchased at a local convenience store. Tap water samples were collected from various local sources, followed by storage in plastic bottles. Complexometric titration to quantify the Ca^{2+} levels in water samples was performed with NN as the colorimetric indicator and 0.01 N aqueous EDTA titration solution as chelating reagent under strong basic condition using 8 N KOH (detailed experimental procedure provided in the ESI†). For spiking tests using tap water, spiked water samples (added Ca^{2+} levels: 0.3, 0.5, 0.7 mmol L^{-1}) were prepared by mixing as-collected tap water with aqueous Ca^{2+} standard solutions in a 99 : 1 (v/v) ratio.

Results and discussion

Optimisation of distance-based Ca^{2+} assays

A preliminary experiment revealed that 20 printing cycles (*i.e.* the amount of nano-optodes deposited with an inkjet printer) of the nano-optode ink was sufficient to obtain visual colorimetric changes (refer to the ESI and Fig. S4† for the detailed experimental procedure and results). Notably, the hydrophobic wax barriers defining the fluidic structure of the devices were not affected by the pre-deposited surfactant (nano-optode sus-
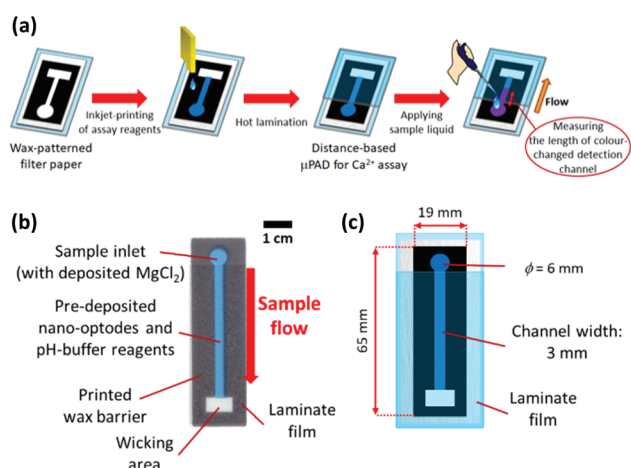
Fig. 1 (a) Schematic procedure of device fabrication by printing technology and Ca^{2+} assay with a Ca^{2+}-selective distance-based µPAD; (b) design of distance-based µPAD for nano-optode based Ca^{2+} detection, and (c) corresponding dimensions representing the settings in the PowerPoint graphic software.

pension), since no leakage of applied sample liquid was observed (refer to the ESI and Fig. S5† for the detailed experimental procedure and results). Whereas manual deposition of nano-optode suspension by pipetting causes the occurrence of a coffee-ring effect after the evaporation of the water solvent,[35] inkjet-dispensed nano-optodes exhibit well-defined and homogeneous optode areas on the surface of the paper substrate (Fig. 2a and b). The printed nano-optodes mainly reside in the filter paper within a depth of approximately 120 μm from the printed surface, as seen in the cross-sectional microscope image shown in Fig. 2c. Additionally, the advantageous capabilities of the filter paper substrate, such as its high porosity and surface area, were maintained for the unhindered liquid wicking character of the original hydrophilic substrate.

The appropriate amounts of chemical reagents for distance-based Ca^{2+} assays (e.g. pH-buffering reagents, pre-deposited $MgCl_2$ salt) were investigated. First, the influence of the amount of deposited pH-buffering reagents (250 mmol L^{-1} HEPES-TMAOH buffer at pH 7.0) was evaluated. For this purpose, 4 different numbers of printing cycles (1, 2, 3 and 5 cycles) were tested with distance-based μPADs (results shown in Fig. S6†). The deposition of two or more printing cycles of the pH-buffer solution resulted in a high background signal indicated by the magenta colour observable also in the absence of Ca^{2+}. This is probably because an excess quantity of cationic buffer components (i.e. TMA^+) affects the cation-exchange reaction of the nano-optodes by an uptake of buffer cations into the nano-optode phase and hence, the deprotonation of chromoionophore even in the absence of target cations. Therefore, one single printing cycle was selected as the optimal amount of deposited pH-buffering solution in device fabrication. Next, the effect of the amount of deposited $MgCl_2$ for improved sensitivity of μPADs was studied (refer to Fig. S7† for the quantitative response curves). In this work, $MgCl_2$ was

deposited in the inlet area to compete in the non-specific interaction between the target cations (Ca^{2+}) and the cellulosic surface during capillary force-driven sample wicking, which results in improved sensitivity for the distance-based Ca^{2+} assay. The reason for this is further explained in the section discussing the interference study. $MgCl_2$ has been selected because the used Ca^{2+} ionophore has excellent selectivity against Mg^{2+},[41] so that the presence of this cation does not contribute to a colorimetric signal. The experimental results of Fig. S7† show that the response curves for Ca^{2+} are vertically shifted towards longer colour-changed distances with increasing amounts of printed $MgCl_2$. However, excess amounts of deposited $MgCl_2$ (i.e. over 5 printing cycles) resulted in a high background signal upon the corresponding μPADs being exposed to the blank and 1 mmol L^{-1} of Ca^{2+} samples (refer to Fig. S8†), due to the extraction of Mg^{2+} into the Ca^{2+}-selective nano-optodes. Therefore, three printing cycles were selected as the appropriate amount of deposited $MgCl_2$ in subsequent experiments.

Distance-based Ca^{2+} assay

To confirm the distance-based colorimetric response of the developed μPADs, aqueous Ca^{2+} samples of various concentrations have been applied onto the paper devices (Fig. 3). The developed μPADs showed a good correlation between the concentration of Ca^{2+} and the length of the colour-developed nano-optode channel in the concentration range of 0–5.0 mmol L^{-1} (Fig. 3), making them ideally suited for the quantification of Ca^{2+} in drinking water samples according to the WHO (less than 5 mmol L^{-1}) and International Organization for Standardization (0.05–2.5 mmol L^{-1}) established recommendations. The batch-to-batch reproducibility of distance-based μPADs has been estimated by using response curves obtained with μPADs independently prepared on different days (Fig. 4a). This data, together with the Pearson's correlation analysis ($r = 0.995$–0.998) comparing the different batches with each other (Fig. S9†), confirms the high fabrication reproducibility of distance-based paper devices, which were independently fabricated on different days. For achieving calibration-free Ca^{2+} quantification by simply relying on a single colour-changed distance measurement, this batch-to-batch reproducibility is one of the most critical criteria for the successful practical application of μPADs. Additionally, it was also experimentally confirmed that the response curve obtained with the aid of scanned images and digital colour analysis shows no significant difference from naked-eye visual readout by independent untrained volunteer users (Fig. 4b). The corresponding Pearson's correlation analysis is summarized in Fig. S10.†

To address the analytical capabilities of the μPADs, the lowest naked-eye detectable concentrations were compared with those achieved with commercial colorimetric paper dipsticks. The assay procedure applied for commercial paper dipsticks and the colorimetric changes corresponding to various Ca^{2+} concentrations are shown in Fig. S11.† In this study, the LOD was defined as the lowest concentration observable by
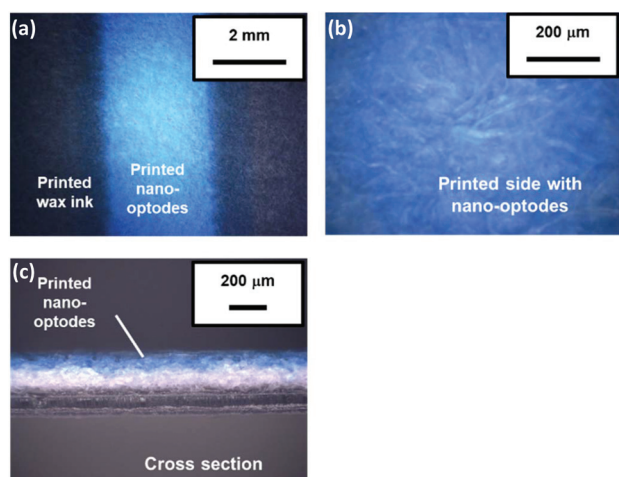
Fig. 2 Microscope images of nano-optode filter paper substrates: (a) nano-optode modified paper surface of the flow channel; (b) scale-up of the nano-optode modified paper surface; and (c) cross section of nano-optode modified paper.
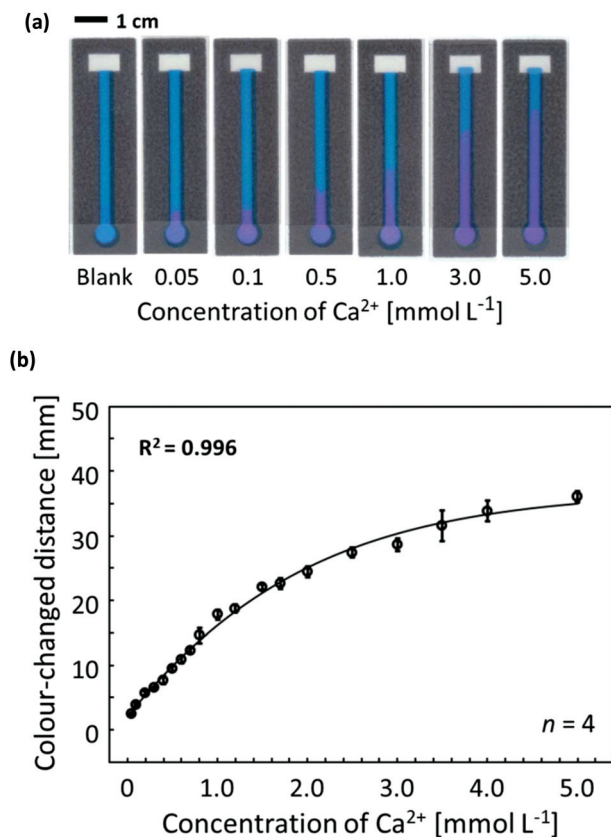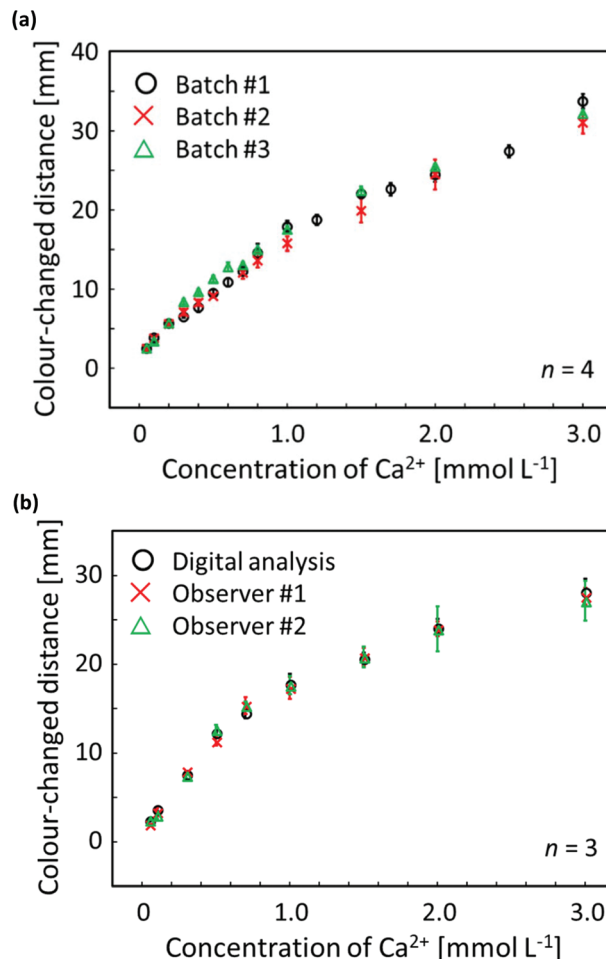
Fig. 3 (a) Scanned images of colour-developed µPADs after application of the corresponding Ca^{2+} solutions of various concentrations (30 µL of aqueous CaCl$_2$); (b) software-assisted response curve of a µPAD-based Ca^{2+} assay; the response curve represented by the solid line was obtained with a non-linear curve fit: $y = -124 + \dfrac{165}{1 + \exp\left(-\dfrac{x - 2.21}{1.99}\right)}$; each data point has been obtained by measurements with 4 individual single-use devices; 30 µL of aqueous CaCl$_2$ solution applied; error bars indicate the standard deviations; incubation time: 45 min.

Fig. 4 (a) Reproducibility evaluation of distance-based µPADs independently fabricated on different days for software-assisted Ca^{2+} quantification; each data point has been obtained by measurements with 4 individual single-use devices; 30 µL of aqueous CaCl$_2$ solution applied; error bars indicate the standard deviations; incubation time: 45 min; circle plots (batch #1) are identical to the data of Fig. 3b; (b) response curves for distance-based Ca^{2+} detection obtained by scanner and software-assisted digital colour analysis (circles) and individual user naked-eye readout (crosses and triangles); each data point has been obtained by measurements with 3 individual single-use devices; 30 µL of aqueous CaCl$_2$ solution applied; error bars indicate the standard deviations; incubation time: 45 min.

naked eye as a visual colour change instead of the classical 3σ method, since a blank sample does not generate any optical signal on distance-based µPADs (*i.e.* blank signal distance = 0 mm). From Table S1,† it can be concluded that the developed distance-based µPADs resulted in lower LOD (0.05 mmol L^{-1}) than commercial colorimetric paper dipsticks for the Ca^{2+} assay shown in Fig. S11† (0.1 mmol L^{-1}). Furthermore, it should be noted that commercial paper dipsticks require a multi-step procedure, including sample pretreatment by reagent addition (Fig. S11a†). Thus, the distance-based µPADs represent sensitive and user-friendly tools for the instrument-free and single-step determination of Ca^{2+} concentrations.

Despite their improved sensitivity for selective naked-eye determination of Ca^{2+} in mineral or tap water, the proposed distance-based paper devices require a relatively long assay time (45 min) to acquire the quantitative optical signal. It is a general drawback that distance-based detection motifs need a prolonged time for assay completion due to the slow transport

of sample liquid by capillary force: up to 45 min have also been reported by others for several centimetres of detection channel length.[16,17,20] In addition, distance-based colorimetric signalling relies on analyte depletion during sample transport, either by binding to a specific receptor[16] or by interaction with the paper substrate, as it is the case in the current work. This can only be achieved with sample liquids being slowly transported through the cellulose fibre network of the paper substrate.

On the other hand, the distance-based colorimetric signal achieved with the present system is stable over time (up to approximately 2 h) so that a user is not forced to continuously monitor the device during an assay, which allows for so-called

"walk-away assays" that require nothing more than the application of the sample. While it is clear that in general a more rapid assay time is desirable, the 45 min assay time is not hindering practical use of the proposed devices. A possible perspective to reduce assay times is the shortening of flow channels. However, this would result in narrowing of the dynamic response range and reducing the signalling resolution. Alternatively, converting a colour intensity-based approach into a distance readout referred to as "dip-and-read distance-based assay" as we have recently reported,[20] might allow nearly instantaneous signal detection, although probably at lower resolution. Furthermore, dipping time dependent result variations would have to be expected, due to the dissolution of buffer salts required for maintaining a constant pH value.

Interference study on distance-based Ca^{2+} assay

The selectivity of the Ca^{2+}-selective µPADs has been qualitatively validated by using aqueous samples of various metal cations (Na^+, K^+, Li^+, Mg^{2+}, Zn^{2+}, Cu^{2+}, Ni^{2+}, Hg^{2+} and Al^{3+}). In this assay, different concentrations of each interfering ion were evaluated on the µPADs and scanned images of devices exposed to the corresponding cation samples are shown in Fig. S12.† Table 1 lists the experimentally evaluated maximal concentrations of interfering ions that do not result in a visually recognizable development of a colour-changed area. Such tolerance against potentially interfering cations (e.g. Na^+, K^+, Mg^{2+}) is comparable to the performance of plasticised PVC-based ISOs using the same ionophore.[41] Additionally, a competitive assay was performed by quantifying the concentration of Ca^{2+} (1 mmol L^{-1}) in the presence of a mixture of Na^+ or Mg^{2+} in aqueous solution (refer to the ESI and Fig. S13†). The colour-changed distance was slightly extended by the presence of these cations at concentrations above 3 mmol L^{-1} or 1 mmol L^{-1} for Na^+ or Mg^{2+}, respectively. It is assumed that changes in the colour-changed distance in mixed sample solutions containing Na^+ or Mg^{2+} are not caused by a lack of selectivity of the nano-optodes on the paper substrate, as confirmed by the data in Table 1. As others have already reported,[35] elevated ionic strengths of samples potentially cause a corresponding increase in viscosity with a decrease in flow velocity, resulting in the extension of length-based signals. However, the amounts of added cations (Na^+ or Mg^{2+}) in the current work are rather unlikely to result in an increase in the viscosity of the applied sample liquid.[35] Therefore, the presence of 1 mmol L^{-1} or higher Mg^{2+} or 3 mmol L^{-1} or higher Na^+ is assumed to cause an extended colour-changed distance mainly due to increased competition for anionic binding sites on the paper surface between the Ca^{2+} target analyte and the other cations, as further outlined below.

It is postulated that the adsorption of Ca^{2+} to the paper substrate is the primary cause for the analyte concentration-dependent changes in colour-changed distance, rather than the depletion of the target cation by extraction into the optode phase. To verify this hypothesis, various concentrations of pH-buffered Ca^{2+} samples were applied onto a reagent-free paper channel, and Ca^{2+}-selective nano-optodes were inkjet-printed onto the µPADs only after exposure to Ca^{2+} samples (refer to the ESI and Fig. S14† for the detailed procedure and the quantitative response curve). The data of Fig. S14† clearly shows that a Ca^{2+} concentration dependent colour-changed length is achieved also in the absence of nano-optodes during sample flow through the detection channel. Hence, it can be concluded that distance-based quantification in this work relies on the non-specific adsorption of Ca^{2+} onto the paper substrate. It is known that the degree of cation transport is modulated by the presence of ionisable sites on cellulosic paper surfaces (mostly carboxyl groups).[29,30,42] A significant amount of carboxyl groups (mmol kg^{-1} order[29,43]) is produced by oxidation of cellulosic hydroxyl groups during the industrial paper making process.[44] Therefore, the surface of filter paper is negatively charged as demonstrated in previously reported articles.[33,45] The electrostatic interaction between a cationic analyte (e.g. Ca^{2+} in this work) and the anionic paper surface results in the adsorption of target cations onto the filter paper surface.[42,46,47] In this adsorption process, the pre-deposited Mg^{2+} competes with the Ca^{2+} analyte for the available binding sites on the paper surface. In addition, the adsorption of metal cations, which is described by a Langmuir adsorption isotherm model, is affected by the ionic strength of the sample liquid.[48] Since the pre-deposited Mg^{2+} also contributes to an increase in ionic strength of the flowing liquid, this leads to decreased adsorption of metal cations onto the paper surface. The pre-deposited Mg^{2+} provides a relatively high but constant ion background, in order to avoid undesired modulation in non-specific Ca^{2+} adsorption due to sample-induced, non Ca^{2+}-related competition for binding sites or changes in ionic strength. The tolerance against interfering cations relies on the total amount of ionised electrolytes (i.e. pH-buffering reagents, $MgCl_2$ on the sample inlet). For drinking or natural water assays, the WHO guideline addresses the threshold values for multiple ions, including those potentially interfering with the current Ca^{2+} assay. The values of taste or health-based thresholds are all well below the amounts that can be tolerated by the developed µPAD[1] and are therefore expected not to interfere with the distance-based Ca^{2+} assay.

Ca^{2+} assays in mineral and tap water samples

The practical applicability of the developed distance-based µPADs was investigated by determining Ca^{2+} levels in mineral water or tap water samples without any sample pretreatment.

Table 1 Tolerance levels for potentially interfering cations

Interfering ions	Tolerance [mmol L^{-1}]	Interfering ions	Tolerance [mmol L^{-1}]
Na^+	100	Cu^{2+}	1000
K^+	100	Ni^{2+}	100
Li^+	100	Hg^{2+}	100
Mg^{2+}	100	Al^{3+}	1000
Zn^{2+}	1		

Cl^- was used as counter anion for preparation of all samples.
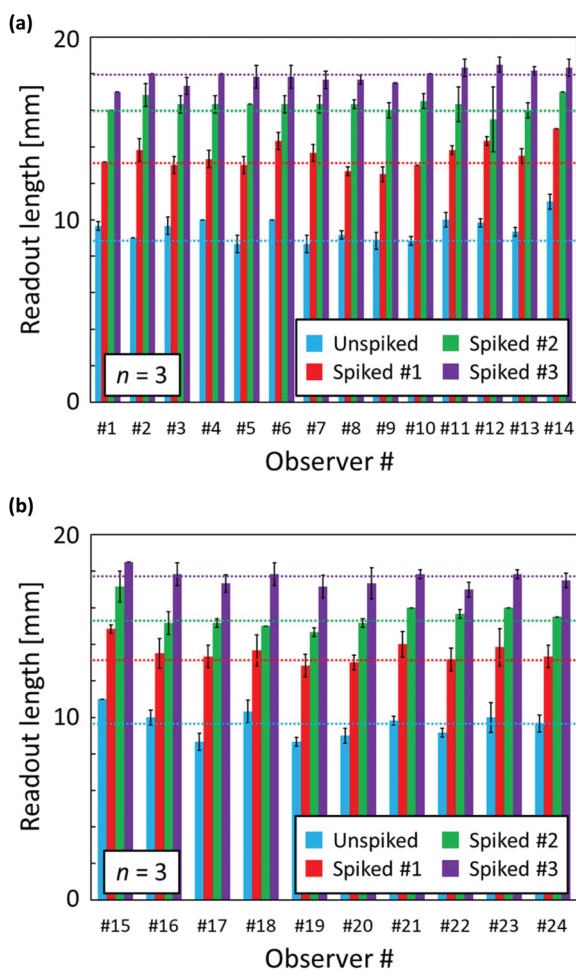
Table 2 Determination of Ca²⁺ concentrations in mineral or tap waters with distance-based µPADs and classical complexometric titration

Sample	Distance-based µPADs[a] (mmol L⁻¹)	Complexometric titration[b] (mmol L⁻¹)	Error[c] (%)
Mineral water			
#1	0.43 ± 0.03	0.43 ± 0.01	0
#2	0.25 ± 0.03	0.23 ± 0.01	+6
#3	0.21 ± 0.02	0.21 ± 0.01	+2
#4	1.96 ± 0.13	2.05 ± 0.01	−5
Tap water			
#1	0.46 ± 0.03	0.41 ± 0.02	+10
#2	0.48 ± 0.03	0.45 ± 0.01	+6
#3	0.51 ± 0.03	0.44 ± 0.01	+15
#4	0.39 ± 0.01	0.35 ± 0.01	+12

[a] Each data has been obtained by measurements with 4 individual single-use devices. [b] Each data has been obtained by 3 individual titrations. [c] Error estimated by comparing with the experimental results obtained by complexometric titration as reference values.

Fig. 5 Naked-eye observer readout of length of colour-changed detection channels from distance-based µPADs after Ca²⁺ assays of a tap water sample; different batches of µPADs were used for data shown in panels (a) and (b); the data represent the mean and standard deviations of 3 independent readouts by 24 observers; the corresponding colour-change lengths obtained with the aid of scanned images and digital colour analysis are indicated by the dotted horizontal lines with a colour corresponding to the legend.

Table 2 summarises the concentrations of Ca²⁺ measured with µPADs and the classical complexometric titration method, with an intermethod result agreement ranging from +15% to −5%. The Pearson's correlation analysis (Fig. S15a†) and the Bland–Altmann method comparison plot (Fig. S15b†) indicate a good agreement between the two independent methods and confirm the suitability of the µPAD for reliable determination of Ca²⁺ levels in real water samples. In the case of Ca²⁺ analysis using mineral water sample #4, the observed standard deviation (Table 2) was slightly higher than for other samples, due to lower device sensitivity in the higher concentration range. For the same reason, the corresponding sample is found outside the 95% limit of agreement in the Bland–Altmann plot of Fig. S15b.† Notably, the distance-based µPADs allow to detect low Ca²⁺ concentration levels (mmol L⁻¹ order), which are out of reach for recently published colorimetric µPADs that do not use optical signal readout instruments.[22]

To further investigate the capability of the distance-based µPADs, quantification of Ca²⁺ levels in spiked tap water samples was carried out by multiple independent observers. The as-collected tap water (tap water #4 shown in Table 2) as well as 3 spiked samples were applied onto µPADs and the resulting length of the colour-changed detection channel was measured by a ruler with sample exposed µPADs presented to observers in a random order. Before testing, the volunteers were instructed on the readout method using one example of a colour-changed µPAD. Fig. 5 shows the visually read out results for various concentrations of Ca²⁺ in tap water or spiked tap water samples. Due to the subjective interpretation of the distance-based signals, some differences between individual observers are unavoidable. Overall, the visually detected distance-based signals were within +23% to −11% of the ImageJ software-assisted readout results (Table S2†).

Conclusion

In this study, fully-printed distance-based microfluidic paper-based analytical devices (µPADs) for simple and reliable determination of Ca²⁺ levels by means of ionophore-doped ion-selective optode nanospheres (nano-optodes) have been demonstrated for the first time. Water-dispersible nano-optodes, which no longer require a volatile organic solvent, allowed for simple desktop thermal inkjet printing-based fabrication of µPADs. Highly batch-to-batch reproducible and reliable devices for naked-eye Ca²⁺-selective assays have been obtained. The developed distance-based µPADs have been successfully applied to visual instrument-free quantification of Ca²⁺ in drinking or tap water samples, with no significant differences compared to classical complexometric titration. It has been experimentally shown that the tolerance of the paper-based devices against other potentially interfering cations was sufficient for Ca²⁺ determination in real world water samples. Notably, the µPADs provided improved lowest naked-eye detectable concentrations of Ca²⁺ (0.05 mmol L⁻¹), compared to known colorimetric approaches. Although a relatively long

assay time (45 min) is required to acquire the quantitative optical signal, we believe that our current work contributes to the further development of inexpensive, equipment-free, easy-to-handle, accurate and highly batch-to-batch reproducible analytical devices for on-site quantification of Ca^{2+} and other cations in real samples.

Conflicts of interest

There are no conflicts of interest to declare.

Acknowledgements

References

1 World Health Organization, *Guidelines for Drinking-Water Quality*, World Health Organization, 4th edn.

2 S. N. Zulkifli, H. A. Rahim and W.-J. Lau, *Sens. Actuators, B*, 2018, **255**, 2657–2689.

3 M. I. G. Almeida, B. M. Jayawardane, S. D. Kolev and I. D. McKelvie, *Talanta*, 2018, **177**, 176–190.

4 International Organization for Standardization, ISO 6058:1984, 1984.

5 M. C. Yappert and D. B. DuPre, *J. Chem. Educ.*, 1997, **74**, 1422.

6 A. W. Martinez, S. T. Phillips, M. J. Butte and G. M. Whitesides, *Angew. Chem., Int. Ed.*, 2007, **46**, 1318–1320.

7 A. W. Martinez, S. T. Phillips, B. J. Wiley, M. Gupta and G. M. Whitesides, *Lab Chip*, 2008, **8**, 2146–2150.

8 A. K. Yetisen, M. S. Akram and C. R. Lowe, *Lab Chip*, 2013, **13**, 2210–2251.

9 Y. Yang, E. Noviana, M. P. Nguyen, B. J. Geiss, D. S. Dandy and C. S. Henry, *Anal. Chem.*, 2016, **89**, 71–91.

10 A. Nilghaz, L. Guan, W. Tan and W. Shen, *ACS Sens.*, 2016, **1**, 1382–1393.

11 K. Yamada, H. Shibata, K. Suzuki and D. Citterio, *Lab Chip*, 2017, **17**, 1206–1249.

12 N. A. Meredith, C. Quinn, D. M. Cate, T. H. Reilly, J. Volckens and C. S. Henry, *Analyst*, 2016, **141**, 1874–1887.

13 Y. Lin, D. Gritsenko, S. Feng, Y. C. Teh, X. Lu and J. Xu, *Biosens. Bioelectron.*, 2016, **83**, 256–266.

14 G. Sriram, M. P. Bhat, P. Patil, U. T. Uthappa, H.-Y. Jung, T. Altalhi, T. Kumeria, T. M. Aminabhavi, R. K. Pai and M. D. Kurkuri, *TrAC, Trends Anal. Chem.*, 2017, **93**, 212–227.

15 Y. Xu, M. Liu, N. Kong and J. Liu, *Microchim. Acta*, 2016, **183**, 1521–1542.

16 D. M. Cate, W. Dungchai, J. C. Cunningham, J. Volckens and C. S. Henry, *Lab Chip*, 2013, **13**, 2397–2404.

17 D. M. Cate, S. D. Noblitt, J. Volckens and C. S. Henry, *Lab Chip*, 2015, **15**, 2808–2818.

18 S. Z. Hossain and J. D. Brennan, *Anal. Chem.*, 2011, **83**, 8772–8778.

19 W. Tan, L. Zhang and W. Shen, *ACS Appl. Mater. Interfaces*, 2017, **9**, 42366–42371.

20 K. Yamada, D. Citterio and C. S. Henry, *Lab Chip*, 2018, **18**(10), 1485–1493.

21 M. A. Ostad, A. Hajinia and T. Heidari, *Microchem. J.*, 2017, **133**, 545–550.

22 S. Karita and T. Kaneta, *Anal. Chim. Acta*, 2016, **924**, 60–67.

23 P. Jarujamrus, N. Malahom, S. Puchum, R. Meelapsom, M. Amatatongchai, A. Siripinyanond, S. Chairam and C. Kulsing, *Talanta*, 2018, **183**, 228–236.

24 G. Mistlberger, G. A. Crespo and E. Bakker, *Annu. Rev. Anal. Chem.*, 2014, **7**, 483–512.

25 X. Xie and E. Bakker, *Anal. Bioanal. Chem.*, 2015, **407**, 3899–3910.

26 K. Mikhelson and M. Peshkova, *Russ. Chem. Rev.*, 2015, **84**, 555.

27 E. Bakker, P. Bühlmann and E. Pretsch, *Chem. Rev.*, 1997, **97**, 3083–3132.

28 M. M. Erenas, I. de Orbe-Payá and L. F. Capitan-Vallvey, *Anal. Chem.*, 2016, **88**, 5331–5337.

29 H. Shibata, T. G. Henares, K. Yamada, K. Suzuki and D. Citterio, *Analyst*, 2018, **143**(3), 678–686.

30 Y. Soda, H. Shibata, K. Yamada, K. Suzuki and D. Citterio, *ACS Appl. Nano Mater.*, 2018, **1**(4), 1792–1800.

31 X. Wang, Y. Qin and M. E. Meyerhoff, *Chem. Commun.*, 2015, **51**, 15176–15179.

32 X. Wang, Q. Zhang, C. Nam, M. Hickner, M. Mahoney and M. Meyerhoff, *Angew. Chem., Int. Ed.*, 2017, **56**, 11826–11830.

33 X. Wang, M. Mahoney and M. E. Meyerhoff, *Anal. Chem.*, 2017, **89**(22), 12334–12341.

34 S. A. Ferguson, X. Wang, M. Mahoney and M. E. Meyerhoff, *Anal. Sci.*, 2018, **34**, 45–50.

35 C. T. Gerold, E. Bakker and C. S. Henry, *Anal. Chem.*, 2018, **90**(7), 4894–4900.

36 P. Kassal, M. Sigurnjak and I. M. Steinberg, *Talanta*, 2019, **193**, 51–55.

37 X. Xie, G. Mistlberger and E. Bakker, *Anal. Chem.*, 2013, **85**, 9932–9938.

38 X. Xie, J. Zhai and E. Bakker, *Anal. Chem.*, 2014, **86**, 2853–2856.

39 N. Komuro, S. Takaki, K. Suzuki and D. Citterio, *Anal. Bioanal. Chem.*, 2013, **405**, 5785–5805.

40 K. Yamada, T. G. Henares, K. Suzuki and D. Citterio, *Angew. Chem., Int. Ed.*, 2015, **54**, 5294–5310.

41 P. Bühlmann, E. Pretsch and E. Bakker, *Chem. Rev.*, 1998, **98**, 1593–1688.

42 R. Ota, K. Yamada, K. Suzuki and D. Citterio, *Analyst*, 2018, **143**, 643–653.

43 A. Murphy, B. Gorey, K. de Guzman, N. Kelly, E. Nesterenko and A. Morrin, *RSC Adv.*, 2015, **5**, 93162–93169.

44 R. Pelton, *TrAC, Trends Anal. Chem.*, 2009, **28**, 925–942.

45 K. Yamada, T. G. Henares, K. Suzuki and D. Citterio, *ACS Appl. Mater. Interfaces*, 2015, **7**, 24864–24875.

46 T. D. Duong, M. Hoang and K. L. Nguyen, *J. Colloid Interface Sci.*, 2005, **287**, 438–443.

47 T. D. Duong, M. Hoang and K. L. Nguyen, *J. Colloid Interface Sci.*, 2004, **276**, 6–12.

48 Z. Reddad, C. Gerente, Y. Andres and P. Le Cloirec, *Environ. Sci. Technol.*, 2002, **36**, 2067–2073.